Manroo *et al. Journal of Engineering and Applied Science* (2022) 69:25
https://doi.org/10.1186/s44147-022-00073-9

Journal of Engineering and Applied Science

REVIEWS Open Access

Study on surface modification and fabrication of surface composites of magnesium alloys by friction stir processing: a review

Suhail Ahmed Manroo*, Noor Zaman Khan and Babar Ahmad

*Correspondence:
suhail_06phd17@nitsri.ac.in
Department of Mechanical Engineering, National Institute of Technology, Srinagar, J&K, India

Abstract

Magnesium alloys and their composites are fast replacing aluminum alloys and other materials in the aerospace and automotive industries. Significant progress has been made in the fabrication of these composites to make them materials of choice for these industries. The choice of the fabrication process is crucial to realize the composites with properties that can compete with the materials currently in vogue. Conventional methods of fabrication of magnesium alloys and their composites are seriously limited as they lead to defects such as porosity and particle clustering. Friction stir processing (FSP) is turning out to be a promising fabrication technique to surmount these challenges. The process being a solid state technique is highly amenable to production of surface modified composites with very attractive mechanical and tribological properties. The main factor making FSP attractive is the relative ease of modification of the surface layers and the incorporation of reinforcement particles. The underlying plastic deformation in FSP ensures that the reinforcement particles are incorporated and distributed uniformly throughout the matrix. This paper attempts to review the current status of FSP as a technique of enabling the surface modification and fabrication of surface composites of magnesium alloys. The objective is to summarize the progress made towards the realization of surface-modified magnesium alloys, primarily in two systems, namely, Mg-AZ system and Mg/rare earth system. The operating conditions (and process parameters) and their subsequent effect on mechanical and tribological properties of the fabricated composites are summarized through the consideration of fabrication of three representative systems, viz., Mg-metal oxide (Mg-MO), Mg-metal carbide (Mg-MC), and Mg-carbon nano tube (Mg-CNT) systems.

Keywords: FSP, Surface composites, Magnesium alloys, Process parameters, Mechanical properties, Tribological properties

Introduction

It is well known [1] that the surface properties are a major factor in determining the functional life of a component. Due to the limitations inherent in the fabrication processes, many components made out of metals and their alloys usually possess poor mechanical and tribological properties, such as strength, hardness, corrosion resistance, fatigue, and wear resistance [2].

To improve and enhance these properties, metal matrix composites (MMCs) have been developed in which a secondary phase material is introduced in the primary metal or alloy generally known as matrix in order to enhance the mechanical and tribological properties [3–7]. Magnesium alloys are widely being used in various industrial sectors where weight reduction is a major concern, such as aerospace, automotive, and defence industries. In the context of automotive and aerospace industries, a reduction in weight while preserving the strength has major implications in terms of the reduction in vehicle weight, which consequently leads to a substantial reduction in the amount of fuel consumed. This, in turn, reduces the fuel costs and alleviates the environmental pollution levels. Sustained efforts of researchers [8–10] in this direction have led to the emergence of magnesium based MMCs as the most promising candidate materials. The processes used to fabricate MMCs are usually classified as solid state, liquid state or deposition type methods [11–17]. Among these, the solid state processing is preferred, as there is no phase transformation of material (to liquid phase) involved, due to which no surface defects are produced [18–20].

Since the last two decades, FSP is considered as the most promising solid state processing method for surface modification and fabrication of surface composites [21–26]. Mishra et al., developed the concept of FSP while working on friction stir welding (FSW), and they were remarkably successful in the fabrication of surface composites of 7075 aluminum alloy [27]. In FSP, a tool with two distinct parts, namely, the shoulder and the pin are used. The former is given a rotational motion while the latter is given a simultaneous linear motion. The softening of material takes place due to generation of heat by friction between the tool and work piece. The pin of the tool is inserted completely into the work piece for the uniform mixing of material in the processed zone. Severe plastic deformation that takes place during stirring of the tool results in grain refinement and surface modification, essentially caused by the dynamic re-crystallization of grains [21, 28–33]. In material processing field, FSP is considered a simple and a promising route to fabrication of materials with improved properties. The advantages of the FSP method are summarized in Table 1 and applications of FSP in industry are shown in Fig. 1. For making a surface composite by FSP, the secondary phase material is introduced in the matrix by employing different strategies. In one of the strategies of surface composite fabrication, a groove is made on the work piece surface and closed with a pin-less shouldered tool to prevent ejection of secondary material from the groove during FSP phase particles are than dispersed throughout the processed zone by FSP, thus formation of surface MMC. The mechanism of dispersion of these particles in the matrix during FSP involves the deformation processes such as forging and extrusion and was first explained by Mishra et al., and other researchers [27, 34].

Table 1 Advantages of FSP

S.No.	Area	Advantages	Reference
1	Mettalurgical	Homogenous microstructure	[35, 36]
		Fine grains	[37, 38]
		Fabrication of metal foam	[39, 40]
		Supersaturated grains	[41, 42]
		Solid state method	[21, 43]
		Good dimensional stability	[44, 45]
		Super plasticity	
2	Bio-Medical	Increased bioactivity of metallic implants	[46–48]
		Improved degradation behavior of metallic implants	
		Fabrication of multi-biofunctional materials	
3	Mechanical	Improved fatigue life	[49, 50]
		Better strength and hardness	
4	Tribological	Improved wear resistance	[51, 52]
		Improved corrosion resistance	
		Low coefficient of friction	
5	Energy	Energy efficient (Less energy reqirement than other solid state processing such as diffusion bonding)	[53, 54]
		Decreased pollution levels in light weight aerospace and automotive applications.	
6	Environmental	Simple and green	[21, 55]
		Eliminate wastage of material	
		No harmful gases produced	
7	Safety	No harmful radiations	[56]
		No spatter	

Methods

The magnesium alloys are fast superseding materials like aluminum, titanium etc., due to their higher strength-to-weight ratio [57]. For this reason, the number of studies on FSP have substantially increased in recent years, particularly on development of magnesium alloys consisting of varying different alloying elements so as to improve their mechanical and tribological properties [58, 59]. The properties of these magnesium alloys can be further enhanced by the FSP. The main challenge is that FSP involves a considerable number of process parameters and the effect of these parameters on various properties is, many a times, contradictory in nature. Furthermore, the properties of magnesium MMCs depend mainly on the type of reinforcement particles, size of reinforcement particles, the percentage of reinforcement material added to matrix, bonding between matrix and reinforcement material and distribution of inter-metallic compounds in the matrix. In this brief, the state of the art of magnesium alloy modification through FSP is presented broadly in two systems, viz., Mg-Al-Zn (Mg-AZ) system and the Mg/rare earth system. The state of the art of magnesium-based surface composite fabrication through FSP is presented broadly in three systems viz., magnesium-metal oxide (Mg-MO) system, magnesium-metal carbide (Mg-MC) system, and magnesium-carbon nano tube (Mg-CNT) system.

Fig. 1 Applications of FSP in Industry

Mg-AZ system

In this system, the surfaces of aluminum and zinc (AZ-series) magnesium alloys such as AZ31, AZ61 and AZ91 are modified through FSP and same is shown in Table 2. $Mg_{17}Al_{12}$ is a general appearing reinforcing phase of Mg-AZ system due to the presence of *Al*% and the amount of zinc [60–63]. The heat of formation of this phase is − 4.36 kj/mol which means that this reinforcing phase is existing stably in the Mg-AZ system [64, 65]. But the coarse eutectic $Mg_{17}Al_{12}$ phase at the grain boundaries is susceptible to instigate cracks under low stress during tensile deformation, thus leads to decrease in mechanical properties of material [66]. Due to FSP, breaking of $Mg_{17}Al_{12}$ takes place and is completely dissolved in the magnesium matrix which results in micro structural modification and homogenization of grains [66, 67].

As per literature FSP is found to be the most promising method of producing fine-grained magnesium alloys [68, 69]. Various researchers also worked on processing of Mg-AZ system by underwater FSP, also known as submerged FSP, and they reported that the resulting microstructure and thus mechanical properties are significantly affected by the surrounding temperature and cooling rate [70]. The submerged FSP is carried under water to provide a better cooling rate as compared to FSP carried in open air. The cooling rate results in decrease of tool wear and time consumed by the processed material above a certain temperature. This suppress the grain growth and as per Hall-Petch relation increase in mechanical properties [71–74]. The multi-pass FSP (MFSP) for Mg-AZ system have also been proven as the most effective FSP technique which results in more grain refinement of the material as compared to single pass FSP. The is because during

Table 2 Brief summary of surface modification of Mg-AZ system alloys by FSP available in the literature

Base material	Tool material	Tool geometry	Tool shape	Process parameters	Significant findings	Ref
AZ31B-H24	H-13	ShD-0.5 inch, PiD-0.25 inch, PiL-0.12 inch	Cylindrical	RS-1200–2000 rpm TS-20–30 in./min	Increase in hardness at low rotational speed and high translational speed.	[75]
AZ31	Steel	ShD-10 mm, PiD-3 mm, PiL-3 mm	Conical pin and concave shoulder	RS-1500 rpm and TS-60 mm/min	1. Grain refinement from 92 μm to 11 μm. 2. Super plasticity o AZ31 with an elongation of 268% at 723 K.	[76]
AZ31	W18Cr4V-Steel	ShD-16 mm, PiD-5 mm, PiL-2.5 mm,	Cylindrical	RS-950 r/min TS-30 mm/min Number of FSP Passes	Two pass FSP leads to more grain refinement (1.2 μm), increase in ultimate tensile strength (82 Mpa) and percentage elongation (11.9%) as compared to single pass (4.2 μm, 43MPa and 4.3%).	[66]
AZ31B-O	Steel	ShD-15 mm, PiD-5 mm, PiL-3 mm	Cylindrical	RS-3000 rpm and 3200 rpm TS-650 mm/min and 550 mm/min Submerged FSP	Submerged FSP leads to more gain refinement in AZ31 alloy by controlling the thermal boundaries of the Process.	[71]
AZ61	Steel	ShD-18 mm PiD-7 mm, PiL-5 mm	Conical	RS-1000 mm/min TS-60 mm/min Number of FSP passes	1. Multiple Pass FSP resulted in more grain refinement (7.8 μm) as compared to single pass FSP (12.5 μm), 2. Increase in tensile properties, strength and ductility.	[77]
AZ61	Steel	ShD-18 mm PiD-4 mm, PiL-6 mm	Cylindrical	1200 r/min TS- 25–30 mm/min Tool tilt angle 1.5^o	1. Nano size grains produced by FSP combined with raPD heat sink. 2. Three times increase in hardness as compared to base material	[78]
AZ61	Steel	ShD-18 mm PiD-16 mm, PiL-8 mm	Concave	RS-500–700 rev/min TS-350 mm/min	Fine grain refinement was observed at 550-600 rev/min. Above this RS the coarser grains were observed.	[79]
AZ91	HCHC-steel	ShD-18and12 mm PiD-5 mm, PiL-3.5 mm	Cylindrical	RS-537 rpm - 900 rpm TS-11.71 mm/min–68.28 mm/min	Optimum tool rotational speed and optimum tool traverse speed for obtaining maximum hardness, minimum corrosion rate and min area surface.	[80]
AZ91	2344-steel	ShD-15 mm PiD-4 mm, PiL-2.5 mm	Cylindrical shoulder and square pin	RS 900 rpm TS-40 mm/min Tilt angle 3^o	1. The nugget or stir zone lies on the advancing side as majority material flow occurs on the advancing side.	[81]

Table 2 Brief summary of surface modification of Mg-AZ system alloys by FSP available in the literature (*Continued*)

Base material	Tool material	Tool geometry	Tool shape	Process parameters	Significant findings	Ref
					2. The width of the stir zone is related to material deformation and micro structure evolution.	
AZ91	Steel	ShD-18 and 12 mm PiD-4 mm, PiL-5 mm and 3 mm	Cylindrical	RS800 rpm TS-60 mm/min Two pass FSP	Two pass FSP leads to more refinement of grains, increase in tensile strength and percentage elongation (312 MPa and 29.4%) as compared to one pass FSP (294 Mpa and 25.2%).	[82]
[83]						

ShD shoulder diameter of tool, *PiD* pin diameter of tool, *PiL* pin length of tool, *RS* rotational speed of tool, *TS* traverse speed of tool, *HCHC* high carbon high chromium[1]

MFSP, $Mg_{17}Al_{12}$ phase is significantly dissolved in magnesium matrix and due to effect of dynamic re-crystallization the micro structure is further refined as shown in Fig. 2a–c [77, 82, 84]. However, attaining optimum pass number is critical as each pass is associated with energy consumption.

Mg/rare-earth system

After Mg-AZ system alloys, Mg/rare earth system alloys are most widely used for several automobile and aerospace applications [85]. The most common alloys of this series are WE43, WE54, and ZE41 and they possess various desirable properties depending upon

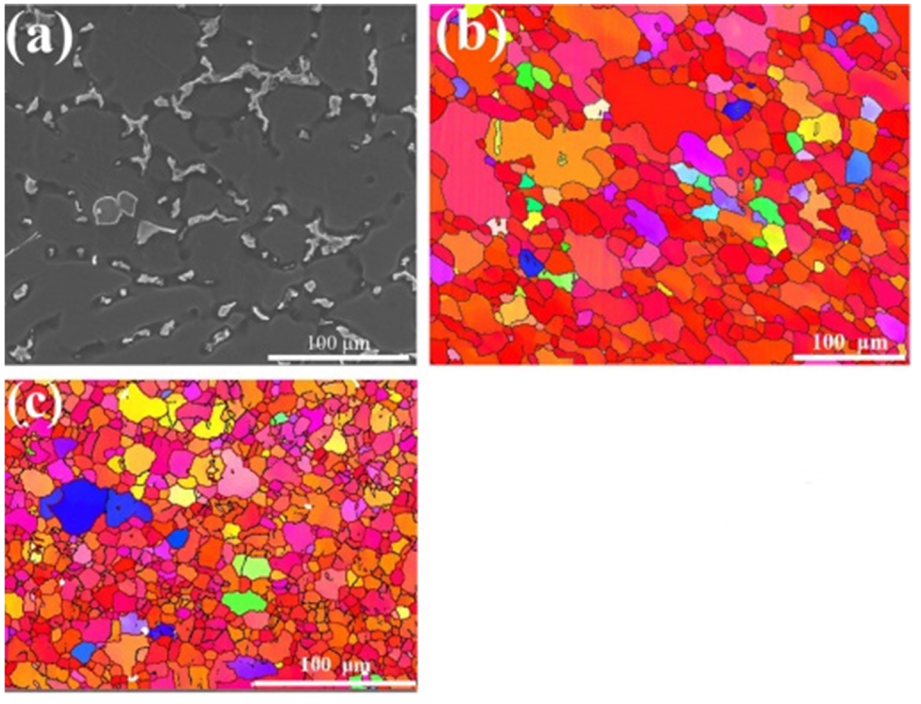

Fig. 2 **a** SEM image of base material **b** EBSD image of single pass FSP and **c** EBSD image of multi-pass FSP [77]

the type of alloying elements added such as Y, Ce, Nd, Gd. The FSP results in fine grain refinement and improved mechanical properties in Mg-Gd-Y-Zr alloy due to complete dissolution of coarse Mg_5(Gd, Y) phase [86, 87]. Palanivel et al. [88] used a modified FSP technique also known as friction stir additive manufacturing to fabricate high strength with considerable ductility WE43 alloys. Their results show fine, uniform, closely populated and well organized precipitates with sizes 2–7nm. Strength of 400 Mpa and 17% ductility of the alloy was also achieved. Venkataiah et al. [45] studied the effect of FSP on the mechanical properties, machining behavior and corrosion rate of ZE41 magnesium alloy. Increase in hardness and decrease in grain size from 110μm to 3μm was achieved after FSP due to the complete dissolution of Mg_7Zn_3RE inter-metallic phase in the matrix. However, they had not observed any change in the corrosion behavior of the alloy after FSP.

Studies on the precipitation behavior of Mg-Y-Nd alloy during FSP were conducted experimentally by Cao et al. [89]. Afterwards, FSPed alloy was aged to modify the microstructure and to investigate the mechanical properties. They achieved grain refinement upto 2.7μm, along with enhanced tensile strength (303 MPa), yield strength (290 Mpa) and elongation (11%) as compared to cast Mg-Y-Nd alloy. Genghua and Zhang Datong [90], processed Mg-Y-Nd alloy by FSP and a tremendous improvement in grain refinement was achieved. The intermetallic phase was observed as $Mg_{12}Nd$ which was completely broken into discontinuous particles by FSP resulting in microstructural modification and hence increase in mechanical properties. Kondaiah et al. [91] studied the effect of FSP process parameters (rotational speed and traverse speed of tool) on micro structural modification and hardness of ZE41 Mg alloy. They reported the formation of super saturated grains, increase in hardness with tool rotational speed and increase in material flow rate during FSP with tool traverse speed. Vasu et al. [92] successfully added calcium (Ca) to ZE41 Mg alloy by FSP targeted for biodegradable implant applications. They achieved a grain refinement up to 7μm due to which the hardness was also increased. They also noticed that with the increase in immersion time, ZE41-Ca composite degrades at a very less rate as compared to unprocessed ZE41 Mg alloy.

Magnesium metal oxide (Mg-MO) system

A summary of suitable metal oxides used with magnesium alloys for producing magnesium MMCs by FSP are given in Table 3.

Mg-Al_2O_3 MMCs

Magnesium on combining with aluminum oxide (Al_2O_3) results in the formation of Mg, MgO, $\gamma - Al_2O_3$, and $Mg_{17}Al_{12}$ phases and is shown in Fig. 3 [93].

As per Mg- Al phase diagram, the dissolution of coarse eutectic $Mg_{17}Al_{12}$ precipitate in magensium matrix requires a heating temperature of 427 °C [94]. Due to slow diffusion rate of aluminum in magnesium matrix, a time duration of approximately 40 h is required for complete dissolution of eutectic $Mg_{17}Al_{12}$ phase in magnesium matrix [95]. But rigorous plastic deformation by FSP and a strain rate up to 0.4% facilitates complete dissolution of aluminum oxide in the magnesium matrix within a short time as during FSP the maximum time that the temperature stays above 200 °C is 25 s [96, 97]. Farji and Asadi [94] produced AZ91-Al_2O_3 MMC by FSP using square and circular tools and the produced composite showed improved hardness and wear resistance. The role of tool rotational

Table 3 Brief summary of Mg-MO surface MMCs by FSP as available in the literature

Base material	Tool material	Tool geometry	Tool shape	Process parameters	Significant findings	Ref
AZ91-Al_2O_3	H-13	ShD-15 mm, PiD-5 mm, Pil-3 mm	circular and square	RS-900 and 1200 rpm TS- 40–80 mm/min Ratio of RS to TS(R/T)	1.Higher R/T ratio and increase in the number of passes results in fine and reduced grains. 2.Increase in hardness and wear resistance occurs by the addition of aluminum oxide (Al_2O_3).	[94]
AZ91D-Al_2O_3	H-21	ShD-20 mm, PiD-4.5 mm, Pil-4.5 mm	Cylindrical	RS-500, 800, 1600, and 2000 rpm TS-20, 40, and & 80 mm/min	1. Addition of nano Al_2O_3 to magnesium matrix increases the hardness by more than 30% as compared to cast magne sium alloy. 2. Additon of Al_2O_3 to AZ91D increases the wear resistance.	[98]
AZ31-Al_2O_3	H-13	ShD-18 mm, PiD-6 mm, Pil-5.7 mm	Cylindrical	RS-800, 1000, and 1200 rpm TS-45 mm/min	Using of threaded pin profile and increase in rotational speed and number of FSP passes leads to better distribution of Al_2O_3 in AZ31 matrix.	[99]
AZ61-SiO_2	Steel	ShD-18mm, PiD-6 mm, Pil-6 mm	Cylindrical	RS-800 rpm TS-45 mm/min Number of passes	1. Four Pass FSP resulted in satisfactory distribution of SiO_2 particles in AZ61 matrix. 2. Refinement of grains up to 0.8 μm is achieved due to the addition of SiO_2 to AZ61 Mg- alloy	[100]
AZ91-SiO_2	H-13	PiD-6 mm, Pil-4 mm,	Cylindrical	RS-1200 rpm TS- 20, 40, & 63 mm/min	Increase in traverse speed results increase in hardness and tensile strength and decrease of grain size in nugget zone.	[101]
AZ31-ZrO_2	H-13	ShD-14 mm, PiD-6 mm, Pil-2 mm	Cylindrical	RS-1250 rpm TS-20 mm/min Number of FSP passes	1. Less agglomeration of ZrO_2 particles in the matrix was seen by increasing number of passses. 2. Increase in shear strain rate from $69s^{-1}$to $88s^{-1}$ after addition of ZrO_2 to magnesium matrix.	[102]
AZ31-ZrO_2	Steel	ShD-16 mm, PiD-4 mm, Pil-3.8 mm	Cylindrical	RS- 1500 rpm TS-50 mm/min	Improved micro-hardness, damping capacity and mechanical properties after addition of ZrO_2 particles to AZ31 Mg- matrix.	[103]

ShD shoulder diameter of tool, *PiD* pin diameter of tool, *Pil* pin length of tool, *RS* rotational speed of tool, *TS* traverse speed of tool[2]

speed and tool traverse speed was an important observation in their study. It was easily understood from their microstructural studies that the lower traverse speed results in better Al_2O_3 particle distribution and less agglomeration as compared to higher traverse speed. This was because the higher traverse speed decreases the rotational speed/traverse speed ratio which leads to poor stirring and mixing of Al_2O_3 in the matrix. The homogenous microstructure was produced with square tool at 900 rpm tool roational speed and 40 mm/min tool traverse speed. Ahmadkhaniha et al. [98] produced AZ91D-Al_2O_3 MMC

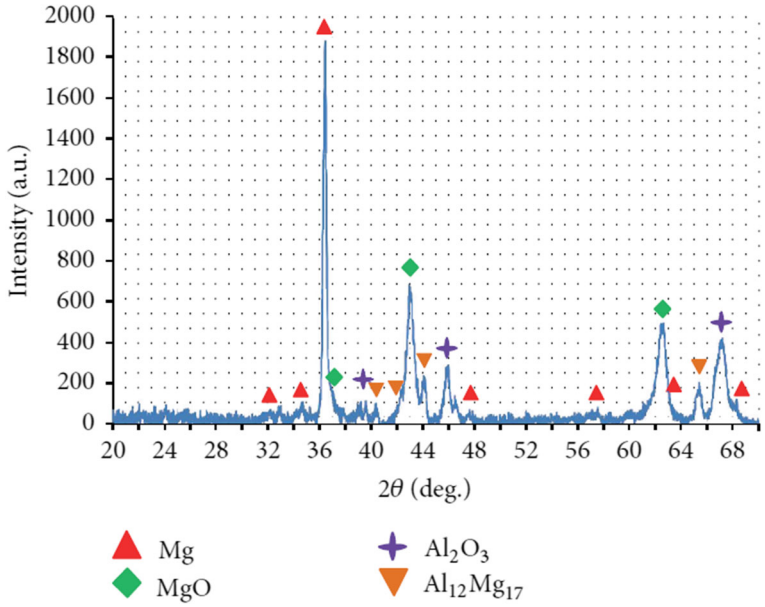

Fig. 3 XRD showing various phases formed after reaction betwen pure Mg and Al_2O_3 [93]

by FSP and demonstrated the effect of the ratio of tool rotational speed and tool traverse speed on the better distribution of Al_2O_3 in the magnesium matrix by FSP. They demonstrated clearly that increase in the tool rotational speed /traverse speed ratio increases the heat and strain of material which resulted in better dispensation and less agglomeration of Al_2O_3 in the magnesium alloy (see Fig. 4). The micro hardness of FSPed AZ91D-Al_2O_3 composite increases to 95 HV as compared to FSPed AZ91 (78HV) without Al_2O_3. This was explained because of the pinning effect of Al_2O_3 particles in the matrix due to which the grain size was significantly reduced and as per Hall-Petch equation, increase in hardness of the material. They also noticed that improved hardness of FSPed specimen with the addition of Al_2O_3 particles limits the deformation and resist the penetration and thus increases the wear resistance.

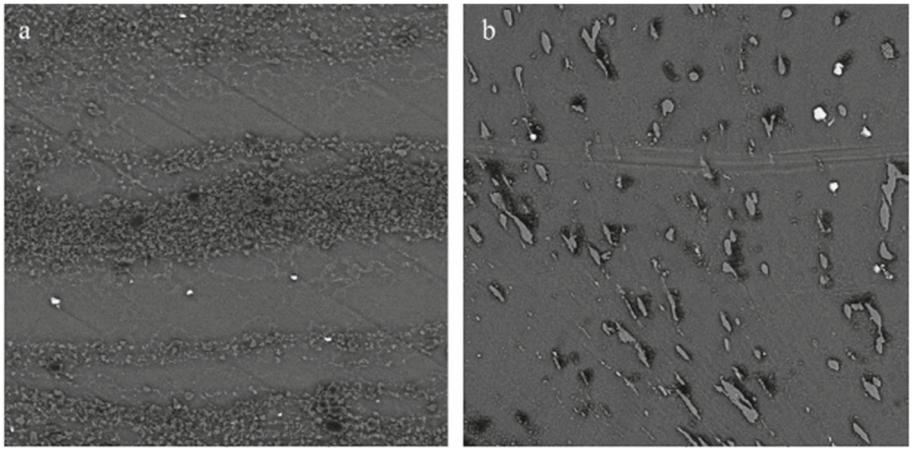

Fig. 4 SEM images of friction stirred AZ91D/Al_2O_3 processed at **a** RS= 800 rpm, TS = 40 mm/min, **b** RS = 800 rpm, TS = 80 mm/min [98]

Azizieh et al. [99] produced AZ31- Al_2O_3 nano composites by FSP using tools with three different pin profiles namely circular pin with no threads, with threads and with threads and three flutes. They studied the effect of rotational speed of tool with constant traverse speed, pin profile and FSP pass number on the distribution of Al_2O_3 in the Mg-matrix. The formation of onion ring type patterns were observed in the micro structures of the composites processed with threaded pin profile at a tool rotational speed of 1000 rpm and 1200 rpm as shown in Fig. 5. The reason behind the formation of onion patterns was explained as improvement in material flow with threaded pin profile due to downward movement of material. They also noticed that the two pass FSP leads to more gain refinement (2.9μm) as compared to single pass FSP (4.4μm). Due to the pinning effect with the addition of Al_2O_3 in the matrix, a grain size of 3.4μm was also achieved.

Abbasi et al. [104] fabricated surface composites on AZ91 magnesium alloy using Al_2O_3 and SiC as reinforcement particles. Their results showed increase in both mechanical and tribological properties of AZ91 magnesium alloy by the incorporation of the reinforcement particles.Their results also showed that samples processed using SiC particles had better mechanical characteristics and corrosion resistance than samples processed using Al_2O_3 particles, although particle type did not have significant effect on wear rate.

Mg-SiO_2 MMCs

Mg-SiO_2 reaction produces Mg_2Si and MgO and is shown by the following reaction [105]

$$4\text{Mg} + SiO_2 = Mg_2Si + 2\text{MgO}$$

The reaction is exothermic and the heat produced in the reaction is responsible to form Mg_2Si and MgO by a self-propagating high temperature synthesis [106]. The formation of intermetallic coarsened Mg_2Si results in degrading the strength and elongation of magnesium alloy. With multi pass FSP, more number of passes will only result in the formation of nano sized phases of Mg_2Si and MgO which are still in fine scale [107]. Khayyamin et al. [101] employed nano SiO_2 with 8% volume fraction in AZ91 magnesium alloy by FSP. The effect of traverse speed and number of FSP passes in the composite fabrication was a key finding in their study. Their micro structural studies revealed the uniform distribution of SiO_2 in the AZ91 matrix with multi pass FSP as compared to single pass FSP. Further, they also observed that increase in traverse speed decreases the grain size and increases the hardness. This is because when the traverse speed is increased, the material

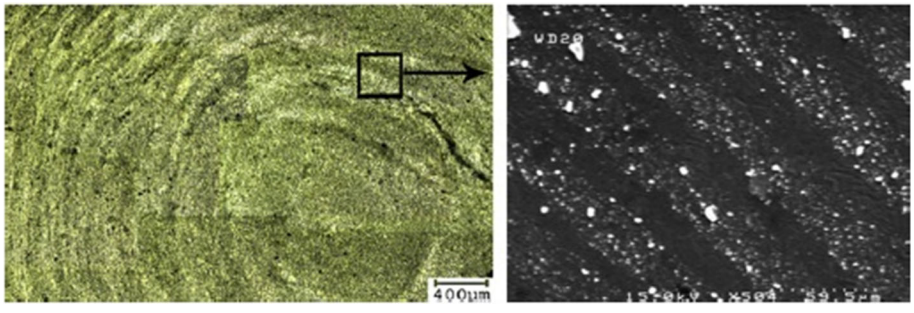

Fig. 5 The onion ring patterns formed with threaded pin profile at 1200 rpm [99]

gets affected by the process heat for a less time which restricts the grain growth during dynamic recrystalization. The maximum hardness of composite was achieved as 124 HV in three pass FSP at a traverse speed of 63 mm/min.

Lee et al. [100] incorporated 5 − 10% nano SiO_2 in AZ61 magnesium alloy matrix using FSP. TEM analysis of their study clearly indicates the formation of Mg_2Si and MgO phases in the matrix as shown in Fig. 6. The authors explained the formation of these phases as a result of reaction between SiO_2 and Mg during FSP. They further concluded that four passes resulted in the uniform distribution of SiO_2 in the matrix and the incorporation of nano SiO_2 paticles in the magnesium matrix increases the hardness to two times as compared to base material.

Mg-ZrO_2 MMCs

On combining ZrO_2 with magnesium there is no new phase formed except for a weak ZrO_2 reinforcement phase. This indicates the stability of ZrO_2 in the magnesium matrix as no intermetallic compound is formed between Mg-ZrO_2 during FSP as shown in the SEM and EDS result of Fig. 7 [107]. Due to plastic deformation during FSP, ZrO_2 particles are distributed uniformly ahead the grain boundaries which restricts the movement of dislocations and results increase in hardness of the processed material [103]. Navazani and Dehghani [102] incorporated ZrO_2 to Mg-matrix by FSP. The mechanical properties were enhanced and fine refinement in grains was observed due to addition of ZrO_2 to Mg - matrix. They observed the enhancement in mechanical properties due to the pinning effect of ZrO_2 particles on the grain boundaries. Further they also observe that multi-pass FSP also improves the pinning effect of particles which results in less agglomeration and fine refinement of particles which is shown in Fig. 8.

Magnesium–metal carbide (Mg-MC) system

In this approach, various metal carbides such as silicon carbide (SiC) and titanium carbides (TiC) are added to magnesium matrix by FSP which is summarized in Table 4.

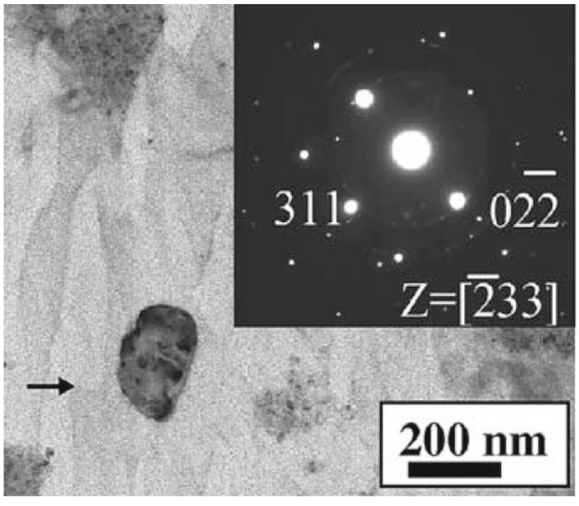

Fig. 6 TEM evidence showing the presence of Mg2Si in the fabricated composite sample [100]

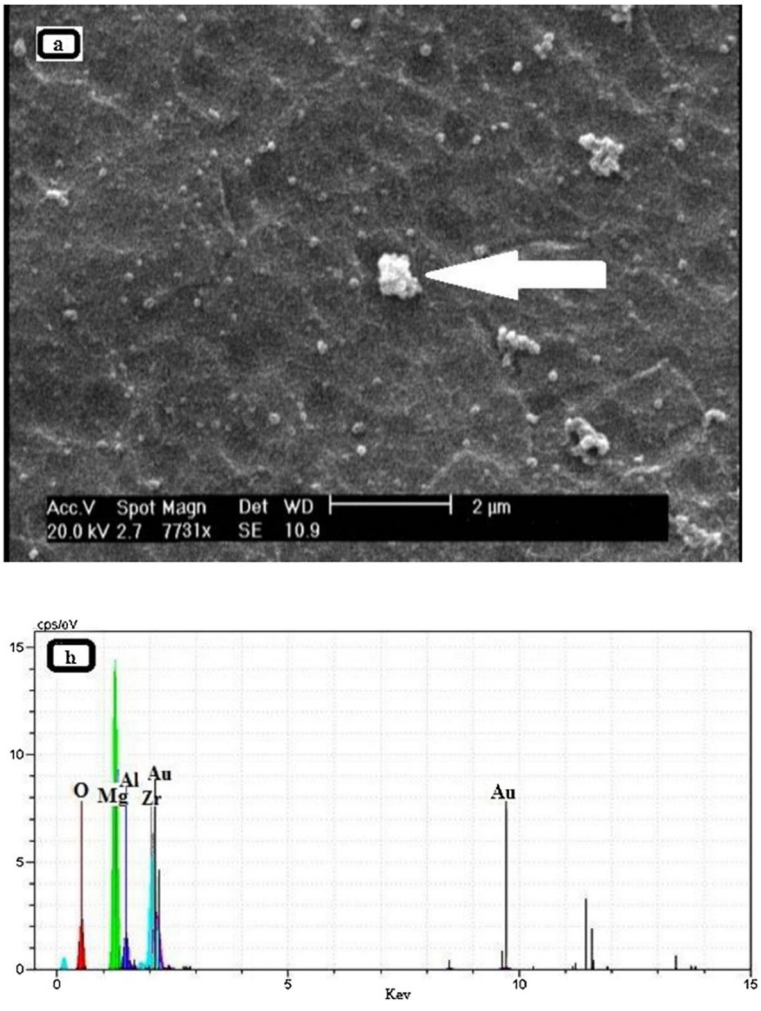

Fig. 7 SEM and EDS images showing dispersion and phases of ZrO_2 in Mg-matrix [102]

Mg-SiC MMCs

Morisada et al. [108] incorporated SiC particles in magnesium AZ31 matrix by FSP and observed the effect of addition of SiC particles on microstructure and hardness of the matrix. They found that addition of SiC to Mg-AZ31 matrix resulted in significant refinement of grains due to severe plastic deformation by tool rotation and pinning effect by SiC particles. Further the change in grain size at the elevated temperatures was also observed. It was seen at above 300 °C temperature, the abnormal grains were formed in FSPed sample without the addition of SiC particles. This resulted in lower hardness values of the processed material due to high temperature generated in the processed region. However the authors found normal and stable grains even at 400 °C by the addition of SiC to AZ31-Mg matrix as shown in Fig. 9.

Erfan and Kashani [109] fabricated the AZ31-SiC composites by incorporating nano SiC particles to AZ31-Mg matrix. They studied the effect of tool tilt angle on performance of composites. It was found that a tool tilt angle of 0° exhibits tunnelling defect in the track during FSP and a tool tilt angle of 3° eliminated tunnelling defect. They also confirmed the better distribution and less agglomeration of SiC particles in the AZ31-Mg

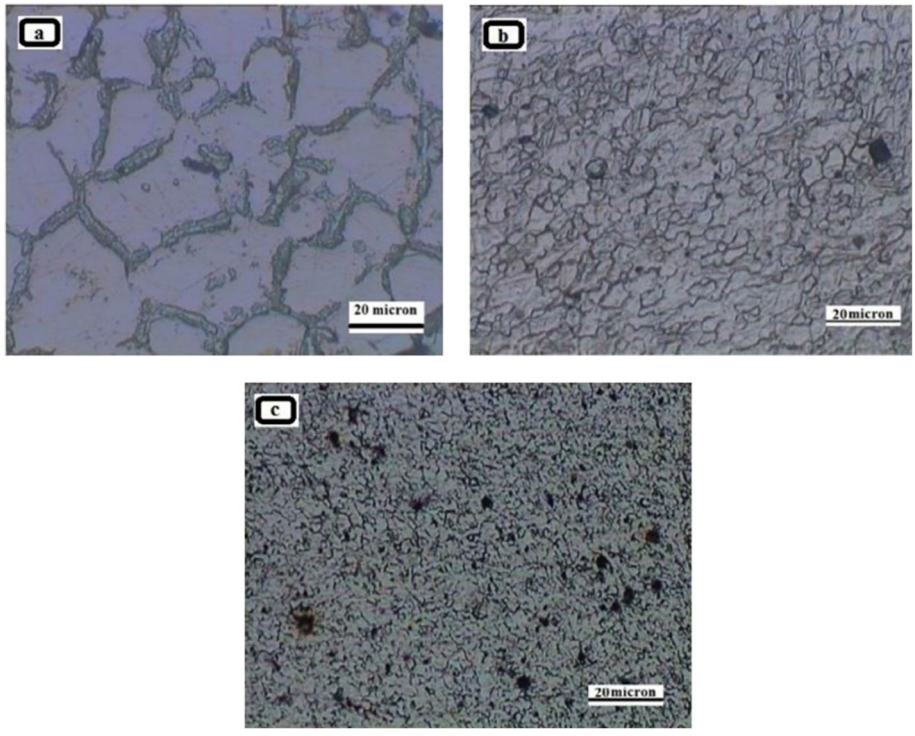

Fig. 8 Effect ofZrO_2 particles and multi pass FSP on microstructure of Mg-matrix [102]

Table 4 Brief summary of Mg-MC surface MMCs by FSP as available in the literature

Base material	Tool material	Tool geometry	Tool shape	Process parameters	Significant findings	Ref
AZ31-SiC	SKD61	ShD-12mm, PiD-4mm, Pil-1.8mm	Cylindrical	RS-1500 rpm TS-25-200 mm/min	1. Addition of SiC to AZ31-Mg matrix leads to refinement of microstructure and increase in hardness to about 80Hv. 2. At elevated temperatures fine grain microstructure produced by FSP of AZ31 Mg-Sic is maintained as compared to fine grain micro structure of AZ31 Mg-matrix produced by FSP without SiC addition.	[108]
AZ31-SiC	H-13	ShD-18mm, PiD-3.4mm, Pil-3mm	Cylindrical	RS-900, 1400, and TS-200, 250, and 1800 rpm 300 mm/min Tilt angles 0° and 3°	1. Increasing the rotational speed /traverse speed ratio and FSP pass number leads to uniform distribution of SiC in magnesium matrix.	[109]
AZ91-SiC	Steel	ShD-15mm, PiD-3.54mm, Pil-2.5mm	Cylindrical	RS-710–1400 rpm TS-12.5–63 mm/min	1. The grain size is increased and hardness is decreased with the increase in tool rotational speed. 2. The grain size decreases and hardness increases by increasing the traverse speed. 3. Multi pass FSP distributes SiC particles uniformly in AZ91-Mg matrix.	[110]

Table 4 Brief summary of Mg-MC surface MMCs by FSP as available in the literature (*Continued*)

Base material	Tool material	Tool geometry	Tool shape	Process parameters	Significant findings	Ref
AZ31-SiC	HSS	SOD-24mm, SID-8mm	Concave	RS-400 rpm TS-30 mm/min	1. Direct FSP (DFSP) results in homogeneous and distributes SiC particles uniformly in one pass only as compared to conventional multi pass FSP. 2. The optimal parameters calculated for uniform distribution of SiC in AZ31-Mg matrix are tool rotational speed = 400 rpm, Tool traverse speed v = 30 mm/min, tool tilt angle=0.5°, and plunge depth d =0.3 mm.	[111]
AZ31-TiC	HCHCr steel	ShD-18 mm, PiD-6 mm Pil-5 mm		RS- 1200 rpm TS-40 mm/min Axial Force- 10 KN	Homogenous distribution of TiC particles in the magnesium matrix without any inter-facial reaction and formation of clusters.	[112]

ShD shoulder diameter of tool, *PiD* pin diameter of tool, *PiL* pin length of tool, *RS* rotational speed of tool, *TS* traverse speed of tool, *HCHC* high carbon high chromium[3]

matrix with the increase in tool rotational speed to tool traverse speed ratio. Asadi et al. [110] added the SiC particles to AZ91-Mg matrix and studied the effect of its addition on micro-structure and hardness of AZ91-Mg alloy.They investigated the effect of tool rotational speed, tool traverse speed and the number of FSP passes on the quality of fabricated composite. The authors concluded that the increase in tool rotational speed decreases the hardness of the composite due to increase in grain size and decrease in tool traverse

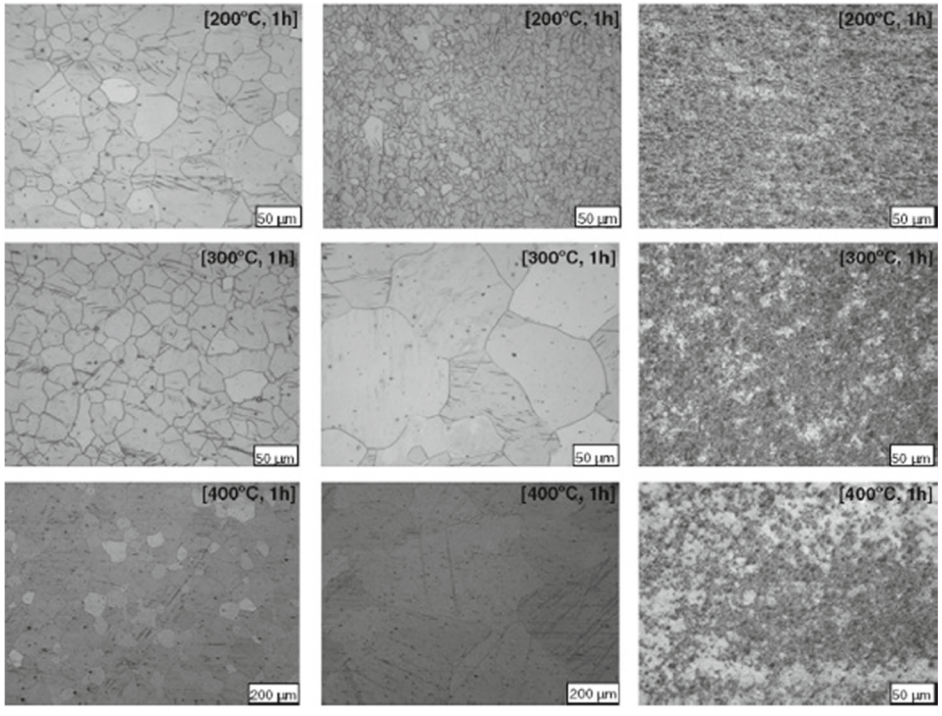

Fig. 9 Micro-structural images of the stir zone after the heat treatment [108]

speed decreases the grain size and increase the hardness of the composite as per hall-Petch equation. Further more they also observed uniform distribution of SiC particles in AZ91 Mg-matrix by multi pass FSP.

Mg–TiC MMCs

TiC is considered as a glamorous reinforcement because of its high elastic modulus, very high hardness and high thermal stability as compared to other ceramic particles [113, 114]. From the work of Balakrishnan et al. [112] it was found that addition of TiC to magnesium matrix by FSP resulted in uniform distribution of TiC particles without undergoing any chemical reaction and the formation of any secondary phase. However their experimental results revealed a complete change in the micro-structure by different volume fractions of TiC used in the Mg- matrix (see Fig. 10). The formula used for calculating the volume fraction is given below

$$\text{Vol. fraction} = (\text{Groove area}/\text{Tool pin area}) * 100 \tag{1}$$

$$\text{Groove area} = \text{Groove width} * \text{Groove depth} \tag{2}$$

$$\text{Tool pin area} = \text{Dia. of pin} * \text{Length of pin} \tag{3}$$

With the increase in volume fration of TiC particles, the spacing between the particles was seen reduced and viceversa.

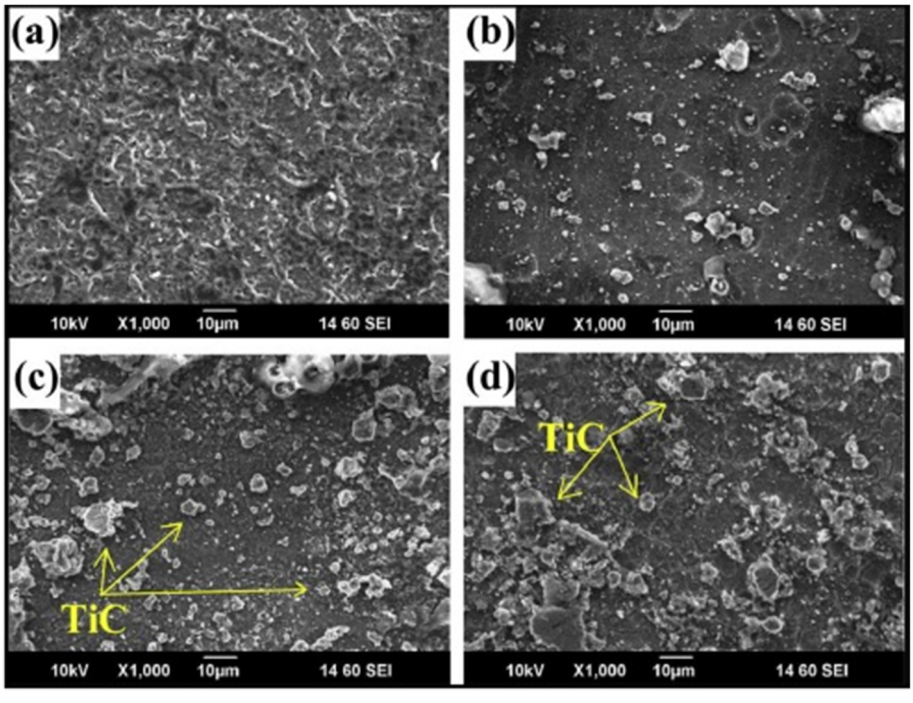

Fig. 10 SEM images of AZ31/TiC composite containing **a** 0 vol.% TiC, **b** 6 vol.% TiC, **c** 12 vol.% TiC, and **d** 18 vol.% TiC [112]

Magnesium carbon nano tubes (Mg-CNTs) system

Carbon nano tubes are considered as an excellent reinforcing material because of their low density, high elastic modulus (1000 GPa) and high tensile strength (50 GPa) [115, 116]. Single walled carbon nano tubes and multi- walled carbon nano tubes (MWCNTs) are generally used depending upon the desired applications [117]. The composites with carbon nano tubes as a reinforcement material formed by the conventional techniques such as casting ([118] and powder metallurgy [119]) resulted in agglomeration and weak bonding at the interface due to which the uniform distribution of these tubes in the matrix becomes difficult. FSP, being a solid state processing technique, can distribute MWCNT's in the matrix uniformly which in turn resulted in improved mechanical, metallurgical and tribological properties and the same is summarized in Table 5 [120].

The uniform distribution along with the morphology of CNTs in Mg-6Zn alloy by FSP was recently reported by Haung et al. [121]. From the TEM results, they observed the singly dispersement of CNTs after FSP without formation of any clusters (see Fig. 11). Their TEM results also confirmed the fecilitation of the sites for nueleation of dynamic recrystilization by incorporation of CNTs. The yeild strength of fabricated composite (Mg-6Zn-CNT) seen was increased to 171Mpa (70 Mpa Mg-6Zn in (cast)), the ultimate tensile strength to 300 Mpa (129 Mpa Mg-6Zn(cast)) and the elongation 15% (8.1% Mg-6Zn in (cast))

Morisada et al. [122] dispersed multiwalled carbon nano tubes (MWCNT's) in AZ31-Mg matrix by FSP and successfully develop a fine-grained composite with hardness twice (78Hv) as compared to that of base metal (41HV). The role of travel speed in the dispersion of MWCNT's in AZ31-Mg matrix was alo a key finding in their study and they concluded that travel speed of 25mm/min resulted in fine and uniform grains by keeping a constant 1500 rpm rotational speed.

The wear behavior of AZ31-Mg alloy with the incorporation of MWCNT's by FSP was studied by Jamshidijam et al. [123]. The addition of MWCNT's to AZ31-Mg increases

Table 5 Brief summary of Mg-MWCNTs surface MMCs by FSP as available in the literature

Base material	Tool material	Tool geometry	Tool shape	Process parameters	Significant findings	Ref
AZ31-MWCNTs	SKD61	ShD-12 mm, PiD-4 mm Pil-1.8 mm	Cylindrical	RS-1500 rpm TS-25–100 mm/min	1. Hardness of AZ31-Mg matrix increases with almost two times due to addition of MWCNTs as compared to base material 2. Fine grains with less than 500 nm can be achieved.	[122]
AZ31-MWCNTs	H-13	ShD-20 mm PiD-4 mm Pil-3 mm	Cylindrical	RS-1500 rpm TS-80 mm/min	1. Increase in wear resistance and hardness with almost double than the base metal with the addition of MWCNTs. 2. Fine grain microstructure.	[123]
AZ31-MWCNTs	Steel	ShD-20 mm PiD-2,4,6,8(PSSC) 0.5,2,3.5,5(PSSS) 5 mm(SC)	Cylindrical	RS-1250 rpm TS-25 mm/min	1. Stepped tools produce fine grains as compared to conventional tools. 2. Uniform and fine grain microstructure micro-structure with higher amount of CNT, low speed ratio and multi-pass FSP.	[124]

ShD shoulder diameter of tool, *PiD* pin diameter of tool, *Pil* pin length of tool, *RS* rotational speed of tool, *TS* traverse speed of tool[4]

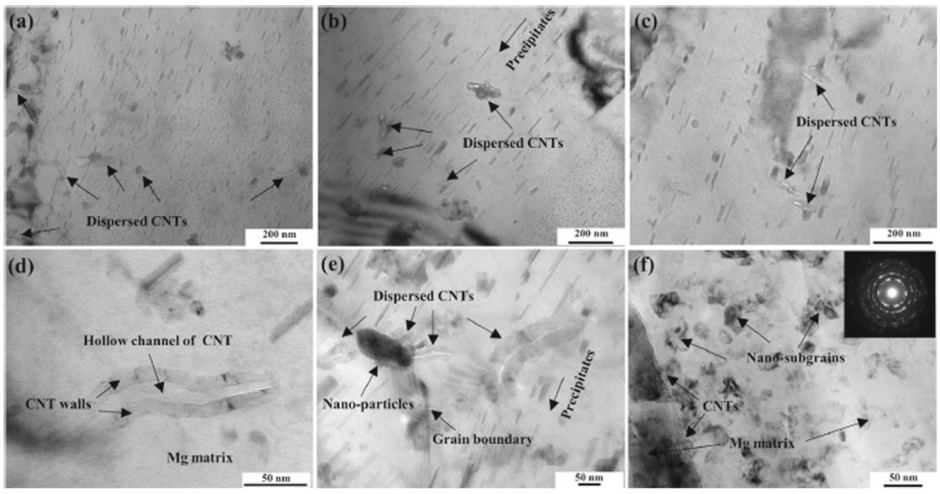

Fig. 11 TEM images of FSPed Mg-CNT MMC: (**a**–**c**) Dispersion of CNTs, (**d**, **e**) CNTs morphology in MMC, (**f**) nano sub grains next to CNT [121]

the wear resistance with almost two times. The grain size was also reduced to 5μm and hardness was increased twice with MWCNT's.

In the work of [124], the effect of different pin profiles of tools along with the speed ratio, number of passes and CNT amount on the quality of developed surface composites were investigated. They noticed a uniform and fine grained micro structure with stepped pin profile, low speed ratio, multi pass FSP, and higher amount of CNT.

Modified friction stir processing techniques

In recent years, several modified methods of FSP have been used to fabricate the surface MMCs and are discussed as follows:

Direct friction stir processing (DFSP)

A modified technique in producing a better surface MMCs without using a pin in the FSP tool also known as direct FSP (DFSP) was firstly reported by Huang et al. [111].

This technique was observed to produce better surface composites in single pass as compared to conventional multi-pass FSP. They used a hollow pin less tool with the outer diameter or shoulder diameter 24 mm and inner diameter 8mm as shown in Fig. 12. Like in conventional FSP, the secondary phase material by DFSP was not preplaced on the base metal but in the hollow portion of the DFSP tool. When the rotating tool traversed in the longitudinal direction of the base metal surface, the secondary phase particles flowed into the encaged space between the base metal plate and the moving shoulder through the hollow space in the tool. Thus, without using a pin, these particles were stirred and pressed into the base metal dispersedly. Therefore, uniform distribution of particle throughout the processed region was successfully obtained with only single pass FSP.

Friction stir vibration (FSVP)

FSP with vibration (FSVP), a novel technique for making surface MMCs was recently introduced by Behrouz Bagheri and Mahmoud Abbasi [125]. The only difference between the two is that in FSVP along with the tool rotational and traverse motions like in FSP

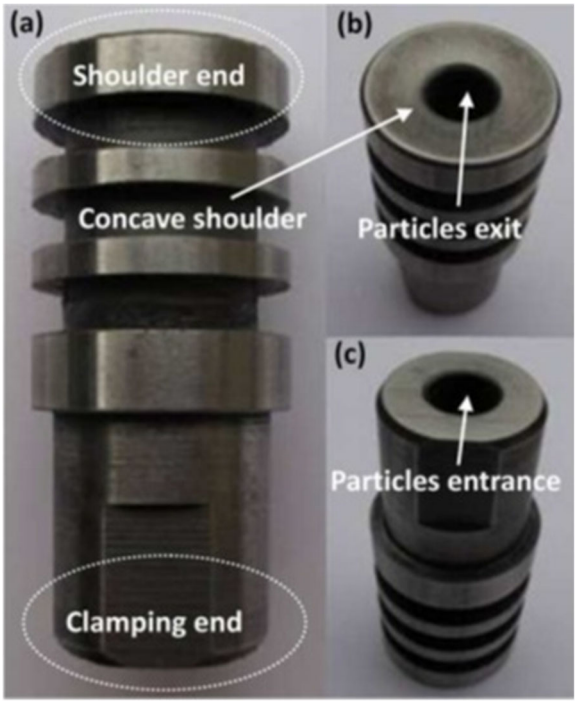

Fig. 12 Images of DFSP tool: **a** front view, **b** shoulder view, and **c** the clamping end [111]

the workpiece is vibrated normal to the processing direction. Their results confirmed the more refinement of grains in FSPV as compared to simple FSP. This was because of the induced vibrations in workpiece during FSP due to which the material deformation was increased which results in breaking of agglomerated reinforcement particles by enhanced dynamic recrystallization.

In another work of Bagheri et al. [126], FSVP was used to fabricate AZ91/SiC surface MMCs. Their microstructural results revealed a better homogenous distribution of SiC particles in AZ91 matrix. Their results also showed more refinement of grains and increase in ultimate tensile strength by FSVP ($(26.43 \pm 2.00)\mu$m and 361.82 MPa) as compared to conventional FSP ($(39.43 \pm 2.00)\mu$m and 324.97 MPa).

Ultrasonic assisted friction stir processing (UaFSP)

Baradarani et al. [127] used the novel UaFSP to enhace the mechanical properties and corrosion resistance of Mg-AZ91 alloy. A remarkable refinement of grains (1.6 μm) with low current density (2.09 $\mu A/cm^2$) was observed with UaFSP as compared to simple FSP. This is due to the fact that due to UaFSP the intermetallic β-Mg_17Al_12 phase was distributed more homogenously in the AZ91 matrix as compared to simple FSP.

Conclusions

In this review paper the basic understanding of enhancement of mechanical and tribological properties with or without the addition of reinforcement particles during FSP of magnesium alloys have been addressed. From this review paper it is concluded that:

1. The mechanical and tribological properties such as tensile strength, hardness, corrosion resistance and wear resistance of magnesium alloys can be improved by

making a surface composite layer of reinforcement particles on magnesium alloys by FSP.

2. The FSP process parameters epecially the tool geometry, i.e., shoulder diameter, pin diameter and pin shape plays an important role in the performance of composite.
3. Selection of optimum tool rotational speed and tool traverse speed in FSP plays a crucial role in producing sound composites of magnesium alloy. Higher tool rotational speed results in better distribution of reinforcement particles across the work piece surface because of more heat generation and more shattering effect of rotation while as low traverse speed results in formation of coarse grains due to increase in material processing time which increases the heat input and results in grain growth. So, obtaining the optimum values of rotational and traverse speed are recommended.
4. Multiple pass FSP results in more grain refinement and uniform distribution of reinforcement particles by accumulating higher degree of strain and dynamic recrystallization.
5. A lot of work has been done on AZ system magnesium alloys as compared to RE system magnesium alloys. It is expected that more number of composites of RE system magnesium alloys will be developed in future by FSP for aerospace, automotive and biodegradable applications.
6. Majority of magnesium metal matrix surface composites are produced using reinforcements of metal oxide system as compared to metal carbide and CNTs system. Its anticipated to produce more number of magnesium surface composites in future by using CNTs system because of its excellent properties as compared to other systems.

Abbreviations
MMC: metal matrix composites; AZ: aluminum and zinc; RE: rare earth; EBSD: electron backscatter diffraction; FSP: friction stir processing; MFSP: multi pass FSP; ShD: shoulder diameter; PiD: pin diameter; PiL: pin length; RS: rotational speed; TS: traverse speed; HCHC: high carbon high chromium; MWCNTs: multi wall carbon nano tube; CNT: carbon nano tube; Al_2O_3: aluminum oxide; SiC: silicon carbide; TIC: titanium carbide; ZrO_2: zirconium oxide

Acknowledgements
Not applicable

Authors' contributions
The research reported in this paper was conceptualized by SAM. The methodology was suggested by BA and NZK. The manuscript was prepared by SAM. BA and NZK supervised the research. All the authors read and approved the final manuscript.

Funding
The authors received no financial support for the research, authorship and publication of this article.

Availability of data and materials
Not applicable.

Code availability
Not applicable.

Declarations

Ethics approval and consent to participate
Not applicable.

Consent for publication
All the authors have consented for publication of the manuscript.

Competing interests
The authors declare that they have no competing of interests.

Received: 20 September 2021 Accepted: 25 January 2022
Published online: 10 March 2022

References

1. Bayoumi MR, Abdellatif A (1995) Effect of surface finish on fatigue strength. Eng Fract Mech 51(5):861–870
2. Besharati-Givi M-K, Asadi P (2014) Advances in Friction-stir Welding and Processing. Elsevier
3. Moustafa EB, Abushanab WS, Melaibari A, Yakovtseva O, Mosleh AO (2021) The effectiveness of incorporating hybrid reinforcement nanoparticles in the enhancement of the tribological behavior of aluminum metal matrix composites. Jom 73(12):1–11
4. Aziz SSA, Abulkhair H, Moustafa EB (2021) Role of hybrid nanoparticles on thermal, electrical conductivity, microstructure, and hardness behavior of nanocomposite matrix. J Mater Res Technol 13:1275–1284
5. Ciach R (2013) Advanced Light Alloys and Composites, vol. 59. Springer
6. Ibrahim I, Mohamed F, Lavernia E (1991) Particulate reinforced metal matrix composites?a review. J Mater Sci 26(5):1137–1156
7. Chung DD (2010) Composite Materials: Science and Applications. Springer
8. Emley E (1966) Principles of magnesium technology pergamon press. Pergamon, New York
9. HASSAN SF (2006) Creation of new magnesium-based material using different types of reinforcements. PhD thesis
10. Hussey RJ, Wilson J (2013) Light Alloys: Directory and Databook. Springer
11. Chawla N, Chawla K (2006) Metal-matrix composites in ground transportation. JoM 58(11):67–70
12. Suresh S (2013) Fundamentals of Metal-matrix Composites. Elsevier
13. Hunt W (1994) Processing and fabrication of advanced materials, the minerals and metal materials society. Warrandale, Warrendale
14. Luo AA, Nyberg EA, Sadayappan K, Shi W (2016) Magnesium front end research and development: a canada-china-usa collaboration. In: Essential Readings in Magnesium Technology. Springer. pp 41–48
15. Hou L, Li Z, Zhao H, Pan Y, Pavlinich S, Liu X, Li X, Zheng Y, Li L (2016) Microstructure, mechanical properties, corrosion behavior and biocompatibility of as-extruded biodegradable mg–3sn–1zn–0.5 mn alloy. J Mater Sci Technol 32(9):874–882
16. Liu H, Cao F, Song G-L, Zheng D, Shi Z, Dargusch MS, Atrens A (2019) Review of the atmospheric corrosion of magnesium alloys. J Mater Sci Technol 35(9):2003–2016
17. Kulekci MK (2008) Magnesium and its alloys applications in automotive industry. Int J Adv Manuf Technol 39(9-10):851–865
18. Chianeh VA, Hosseini HM, Nofar M (2009) Micro structural features and mechanical properties of al–al3ti composite fabricated by in-situ powder metallurgy route. J Alloys Compd 473(1-2):127–132
19. Peng H, Wang D, Geng L, Yao C, Mao J (1997) Evaluation of the microstructure of in-situ reaction processed al3ti-al2o3-al composite. Scr Mater 37(2):199–204
20. Hayes R, Rodriguez R, Lavernia E (2001) The mechanical behavior of a cryomilled al–10ti–2cu alloy. Acta Mater 49(19):4055–4068
21. Mishra RS, Ma Z (2005) Friction stir welding and processing. Mater Sci Eng R Rep 50(1-2):1–78
22. Moustafa EB, AbuShanab WS, Ghandourah E, Taha MA (2020) Microstructural, mechanical and thermal properties evaluation of aa6061/al2o3-bn hybrid and mono nanocomposite surface. J Mater Res Technol 9(6):15486–15495
23. Moustafa EB, Melaibari A, Alsoruji G, Khalil AM, Mosleh AO (2021) Al 5251-based hybrid nanocomposite by fsp reinforced with graphene nanoplates and boron nitride nanoparticles: Microstructure, wear, and mechanical characterization. Nanotechnol Rev 10(1):1752–1765
24. AbuShanab WS, Moustafa EB (2020) Effects of friction stir processing parameters on the wear resistance and mechanical properties of fabricated metal matrix nanocomposites (mmncs) surface. J Mater Res Technol 9(4):7460–7471
25. Dilip J, Ram GJ (2013) Microstructures and properties of friction freeform fabricated borated stainless steel. J Mater Eng Perform 22(10):3034–3042
26. Meng X, Huang Y, Cao J, Shen J, dos Santos JF (2020) Recent progress on control strategies for inherent issues in friction stir welding. Prog Mater Sci 15:2735–2780
27. Mishra RS, Mahoney MW, McFaden SX, Mara NA, Mukherjee AK (1999) High strain rate superplasticity in a friction stir processed 7075 Al alloy. Scr Mater 42(2)
28. Moustafa EB (2021) Hybridization effect of bn and al2o3 nanoparticles on the physical, wear, and electrical properties of aluminum aa1060 nanocomposites. Appl Phys A 127(9):1–9
29. Albakri A, Mansoor B, Nassar H, Khraisheh M (2013) Thermo-mechanical and metallurgical aspects in friction stir processing of az31 mg alloy?a numerical and experimental investigation. J Mater Process Technol 213(2):279–290
30. Khan NZ, Siddiquee AN, Khan ZA, Shihab SK (2015) Investigations on tunneling and kissing bond defects in fsw joints for dissimilar aluminum alloys. J Alloys Compd 648:360–367
31. Gangil N, Maheshwari S, Siddiquee AN (2018) Influence of tool pin and shoulder geometries on microstructure of friction stir processed aa6063/sic composites. Mech Ind 19(2):211
32. Kumar N, Mishra RS, Huskamp C, Sankaran KK (2011) Microstructure and mechanical behavior of friction stir processed ultrafine grained al–mg–sc alloy. Mater Sci Eng A 528(18):5883–5887
33. Siddiquee AN, Pandey S (2014) Experimental investigation on deformation and wear of wc tool during friction stir welding (fsw) of stainless steel. Int J Adv Manuf Technol 73(1-4):479–486
34. Arbegast WJ (2008) A flow-partitioned deformation zone model for defect formation during friction stir welding. Scr Mater 58(5):372–376
35. Hsu C, Kao P, Ho N (2005) Ultrafine-grained al–al2cu composite produced in situ by friction stir processing. Scr Mater 53(3):341–345
36. Santella M, Engstrom T, Storjohann D, Pan T-Y (2005) Effects of friction stir processing on mechanical properties of the cast aluminum alloys a319 and a356. Scr Mater 53(2):201–206

37. Pradeep S, Pancholi V (2013) Effect of microstructural inhomogeneity on superplastic behaviour of multipass friction stir processed aluminium alloy. Mater Sci Eng A 561:78–87
38. Cavaliere P, De Marco P (2007) Friction stir processing of a zr-modified 2014 aluminium alloy. Mater Sci Eng A 462(1-2):206–210
39. Nascimento F, Santos T, Vilaça P, Miranda R, Quintino L (2009) Microstructural modification and ductility enhancement of surfaces modified by fsp in aluminium alloys. Mater Sci Eng A 506(1-2):16–22
40. Charit I, Mishra RS (2003) High strain rate superplasticity in a commercial 2024 al alloy via friction stir processing. Mater Sci Eng A 359(1-2):290–296
41. Ma Z, Mishra RS, Mahoney MW (2002) Superplastic deformation behaviour of friction stir processed 7075al alloy. Acta Mater 50(17):4419–4430
42. El Rayes MM, El Danaf EA, Soliman MS (2011) High-temperature deformation and enhanced ductility of friction stir processed-7010 aluminum alloy. Eng Mater Des 32(4):1916–1922
43. Zhang H (2010) Friction stir welding of magnesium alloys. In: Welding and Joining of Magnesium Alloys. Elsevier. pp 274–305
44. Hangai Y, Nakano Y, Utsunomiya T, Kuwazuru O, Yoshikawa N (2017) Drop weight impact behavior of al-si-cu alloy foam-filled thin-walled steel pipe fabricated by friction stir back extrusion. J Mater Eng Perform 26(2):894–900
45. Venkataiah M, Kumar TA, Rao KV, Kumar SA, Siva I, Sunil BR (2019) Effect of grain refinement on corrosion rate, mechanical and machining behavior of friction stir processed ze41 mg alloy. Trans Indian Inst Metals 72(1):123–132
46. Sezer N, Evis Z, Kayhan SM, Tahmasebifar A, Koç M (2018) Review of magnesium-based biomaterials and their applications. J Magnes Alloys 6(1):23–43
47. Kannan MB, Dietzel W, Zettler R (2011) In vitro degradation behaviour of a friction stir processed magnesium alloy. J Mater Sci Mater Med 22(11):2397–2401
48. Saikrishna N, Reddy GPK, Munirathinam B, Sunil BR (2016) Influence of bimodal grain size distribution on the corrosion behavior of friction stir processed biodegradable az31 magnesium alloy. J Magnes Alloys 4(1):68–76
49. Mishra RS, De PS, Kumar N (2014) Friction stir processing. In: Friction Stir Welding and Processing. Springer. pp 259–296
50. Costa J, Jesus J, Loureiro A, Ferreira J, Borrego L (2014) Fatigue life improvement of mig welded aluminium t-joints by friction stir processing. Int J Fatigue 61:244–254
51. Asl AM, Khandani S (2013) Role of hybrid ratio in microstructural, mechanical and sliding wear properties of the al5083/graphitep/al2o3p a surface hybrid nanocomposite fabricated via friction stir processing method. Mater Sci Eng A 559:549–557
52. Hosseini S, Ranjbar K, Dehmolaei R, Amirani A (2015) Fabrication of al5083 surface composites reinforced by cnts and cerium oxide nano particles via friction stir processing. J Alloys Compounds 622:725–733
53. Thomas W, Nicholas E (1997) Friction stir welding for the transportation industries. Mater Des 18(4-6):269–273
54. Ma Z (2008) Friction stir processing technology: a review. Metall and Mater Trans A 39(3):642–658
55. Mahoney MW, Mishra RS (2007) Friction Stir Welding and Processing. ASM international
56. Sanderson A, Punshon C, Russell J (2000) Advanced welding processes for fusion reactor fabrication. Fusion Eng Des 49:77–87
57. King J (2007) Magnesium: commodity or exotic? Mater Sci Technol 23(1):1–14
58. Srinivasan A, Ajithkumar K, Swaminathan J, Pillai U, Pai B (2013) Creep behavior of az91 magnesium alloy. Procedia Eng 55:109–113
59. CAO L.-j., TANG C.-c., et al. (2012) Effects of isothermal process parameters on semisolid microstructure of mg-8% al-1% si alloy. Trans Nonferrous Metals Soc China 22(10):2364–2369
60. Akyuz B (2014) A study on wear and machinability of az series (az01-az91) cast magnesium alloys. Kov Mater 52:255–262
61. Akyuz B (2013) Influence of al content on machinability of az series mg alloys. Trans Nonferrous Metals Soc China 23(8):2243–2249
62. Candan S, Unal M, Koc E, Turen Y, Candan E (2011) Effects of titanium addition on mechanical and corrosion behaviours of az91 magnesium alloy. J Alloys Compd 509(5):1958–1963
63. Li X-L, Chen Y-B, Xiang W, et al. (2010) Effect of cooling rates on as-cast microstructures of mg-9al-xsi (x= 1, 3) alloys. Trans Nonferrous Metals Soc China 20:393–396
64. Zhou D, Liu J, Xu S, Peng P (2010) Thermal stability and elastic properties of mg3sb2 and mg3bi2 phases from first-principles calculations. Phys B Condens Matter 405(13):2863–2868
65. Zhou D, Liu J.-s., Lu Y.-z., Zhang C.-h. (2008) Mechanism of sb, bi alloying on improving heat resistance properties of mg-al alloy. Chin J Nonferrous Metals 18(1):118
66. Wen W, Kuaishe W, Qiang G, Nan W (2012) Effect of friction stir processing on microstructure and mechanical properties of cast az31 magnesium alloy. Rare Metal Mater Eng 41(9):1522–1526
67. Chang C, Du X, Huang J (2007) Achieving ultrafine grain size in mg–al–zn alloy by friction stir processing. Scr Mater 57(3):209–212
68. Kwon Y, Saito N, Shigematsu I (2002) Friction stir process as a new manufacturing technique of ultrafine grained aluminum alloy. J Mater Sci Lett 21(19):1473–1476
69. Mansoor B, Ghosh A (2012) Microstructure and tensile behavior of a friction stir processed magnesium alloy. Acta Mater 60(13-14):5079–5088
70. Darras BM, Omar M, Khraisheh MK (2007) Experimental thermal analysis of friction stir processing. In: Materials Science Forum, vol. 539. Trans Tech Publ. pp 3801–3806
71. Darras B, Kishta E (2013) Submerged friction stir processing of az31 magnesium alloy. Mater Des 47:133–137
72. Darras BM (2012) A model to predict the resulting grain size of friction-stir-processed az31 magnesium alloy. J Mater Eng Perform 21(7):1243–1248
73. Luo X, Cao G, Zhang W, Qiu C, Zhang D (2017) Ductility improvement of an az61 magnesium alloy through two-pass submerged friction stir processing. Materials 10(3):253
74. SAKURADA D, Katoh K, Tokisue H (2002) Underwater friction welding of 6061 aluminum alloy. Keikinzoku 52(1):2–6

75. Darras B, Khraisheh M, Abu-Farha F, Omar M (2007) Friction stir processing of commercial az31 magnesium alloy. J Mater Process Technol 191(1-3):77–81
76. Zhang D-T, Xiong F, Zhang W-W, Cheng Q, Zhang W (2011) Superplasticity of az31 magnesium alloy prepared by friction stir processing. Trans Nonferrous Metals Soc China 21(9):1911–1916
77. Luo X, Zhang D, Zhang W, Qiu C, Chen D (2018) Tensile properties of az61 magnesium alloy produced by multi-pass friction stir processing: Effect of sample orientation. Mater Sci Eng A 725:398–405
78. Du X-H, Wu B-L (2008) Using friction stir processing to produce ultrafine-grained microstructure in az61 magnesium alloy. Trans Nonferrous Metals Soc China 18(3):562–565
79. Zhou L, Li G, Zha G, Shu F, Liu H, Feng J (2018) Effect of rotation speed on microstructure and mechanical properties of bobbin tool friction stir welded az61 magnesium alloy. Sci Technol Weld Join 23(7):596–605
80. Vignesh RV, Padmanaban R, Govindaraju M (2019) Investigations on the surface topography, corrosion behavior, and biocompatibility of friction stir processed magnesium alloy az91d. Surf Topogr Metrol Prop 7(2):025020
81. Asadi P, Mahdavinejad R, Tutunchilar S (2011) Simulation and experimental investigation of fsp of az91 magnesium alloy. Mater Sci Eng A 528(21):6469–6477
82. Chai F, Yan F, Wang W, Lu Q, Fang X (2018) Microstructures and mechanical properties of az91 alloys prepared by multi-pass friction stir processing. J Mater Res 33(12):1789–1796
83. Argade G, Kandasamy K, Panigrahi S, Mishra R (2012) Corrosion behavior of a friction stir processed rare-earth added magnesium alloy. Corros Sci 58:321–326
84. Feng A, Xiao B, Ma Z, Chen R (2009) Effect of friction stir processing procedures on microstructure and mechanical properties of mg-al-zn casting. Metall and Mater Trans A 40(10):2447–2456
85. Sunil BR (2019) Surface Engineering by Friction-assisted Processes: Methods, Materials, and Applications. CRC Press
86. Xiao B, Yang Q, Yang J, Wang W, Xie G, Ma Z (2011) Enhanced mechanical properties of mg–gd–y–zr casting via friction stir processing. J Alloys Compd 509(6):2879–2884
87. Yang Q, Xiao B, Ma Z (2012) Influence of process parameters on microstructure and mechanical properties of friction-stir-processed mg-gd-y-zr casting. Metall and Mater Trans A 43(6):2094–2109
88. Palanivel S, Nelaturu P, Glass B, Mishra R (2015) Friction stir additive manufacturing for high structural performance through microstructural control in an mg based we43 alloy. Mater Des (1980-2015) 65:934–952
89. Cao G, Zhang D, Luo X, Zhang W, Zhang W (2016) Effect of aging treatment on mechanical properties and fracture behavior of friction stir processed mg–y–nd alloy. J Mater Sci 51(16):7571–7584
90. Cao GH, Zhang DT (2015) Microstructure and mechanical properties of submerged friction stir processing mg-y-nd alloy. In: Materials Science Forum, vol. 816. Trans Tech Publ. pp 404–410
91. Kondaiah V, Pavanteja P, Manvit MM, Kumar RR, Kumar RG, Sunil BR (2019) Surface engineering of ze 41 mg alloy by friction stir processing: Effect of process parameters on microstructure and hardness evolution. Mater Today Proc 18:125–131
92. Vasu C, Durga KN, Srinivas I, Dariyavali S, Venkateswarlu B, Sunil BR (2019) Developing composite of ze41 magnesium alloy-calcium by friction stir processing for biodegradable implant applications. Mater Today Proc 18:270–277
93. Mounib M, Pavese M, Badini C, Lefebvre W, Dieringa H (2014) Reactivity and microstructure of al2o3-reinforced magnesium-matrix composites. Adv Mater Sci Eng 2014:1321–1326
94. Faraji G, Asadi P (2011) Characterization of az91/alumina nanocomposite produced by fsp. Mater Sci Eng A 528(6):2431–2440
95. Kleiner S, Beffort O, Uggowitzer PJ (2004) Microstructure evolution during reheating of an extruded mg–al–zn alloy into the semisolid state. Scr Mater 51(5):405–410
96. Ma Z, Sharma S, Mishra R (2006) Microstructural modification of as-cast al-si-mg alloy by friction stir processing. Metall Mater Trans A 37(11):3323–3336
97. Chang C, Lee C, Huang J (2004) Relationship between grain size and zener–holloman parameter during friction stir processing in az31 mg alloys. Scr Mater 51(6):509–514
98. Ahmadkhaniha D, Sohi MH, Salehi A, Tahavvori R (2016) Formations of az91/al2o3 nano-composite layer by friction stir processing. J Magn Alloys 4(4):314–318
99. Azizieh M, Kokabi A, Abachi P (2011) Effect of rotational speed and probe profile on microstructure and hardness of az31/al2o3 nanocomposites fabricated by friction stir processing. Mater Des 32(4):2034–2041
100. Lee C, Huang J, Hsieh P (2006) Mg based nano-composites fabricated by friction stir processing. Scr Mater 54(7):1415–1420
101. Khayyamin D, Mostafapour A, Keshmiri R (2013) The effect of process parameters on microstructural characteristics of az91/sio2 composite fabricated by fsp. Mater Sci Eng A 559:217–221
102. Navazani M, Dehghani K (2016) Fabrication of mg-zro2 surface layer composites by friction stir processing. J Mater Process Technol 229:439–449
103. POSTOPKOM V-T (2019) Effect of zro2 additions on fabrication of zro2/mg composites via friction-stir processing. Mater Tehnologije 53(2):193–197
104. Abbasi M, Bagheri B, Dadaei M, Omidvar H, Rezaei M (2015) The effect of fsp on mechanical, tribological, and corrosion behavior of composite layer developed on magnesium az91 alloy surface. The Int J Adv Manuf Technol 77(9-12):2051–2058
105. Kondoh K, Luangvaranunt T (2003) New process to fabricate magnesium composites using sio2 glass scraps. Mater Trans 44(12):2468–2474
106. Kondoh K, Oginuma H, Aizawa T (2003) Tribological properties of magnesium composite alloy with in-situ synthesized mg2si dispersoids. Mater Trans 44(4):524–530
107. CI C, YN W, HR P, JC H (2006) On the hardening of friction stir processed mg-az31 based composites with 5–20% nano-zro2 and nano-sio2 particles. Mater Trans 47(12):2942–2949
108. Morisada Y, Fujii H, Nagaoka T, Fukusumi M (2006) Effect of friction stir processing with sic particles on microstructure and hardness of az31. Mater Sci Eng A 433(1-2):50–54
109. Erfan Y, Kashani-Bozorg SF (2011) Fabrication of mg/sic nanocomposite surface layer using friction stir processing technique. Int J Nanosci 10(04n05):1073–1076

110. Asadi P, Besharati Givi M, Faraji G (2010) Producing ultrafine-grained az91 from as-cast az91 by fsp. Mater Manuf Process 25(11):1219–1226
111. Huang Y, Wang T, Guo W, Wan L, Lv S (2014) Microstructure and surface mechanical property of az31 mg/sicp surface composite fabricated by direct friction stir processing. Mater Des 59:274–278
112. Balakrishnan M, Dinaharan I, Palanivel R, Sivaprakasam R (2015) Synthesize of az31/tic magnesium matrix composites using friction stir processing. J Magn Alloys 3(1):76–78
113. Razavi M, Ghaderi R, Rahimipour MR, Shabni MO (2012) Synthesis of tic master alloy in nanometer scale by mechanical milling. Mater Manuf Process 27(12):1310–1314
114. Saba F, Sajjadi SA, Haddad-Sabzevar M, Zhang F (2018) Tic-modified carbon nanotubes, tic nanotubes and tic nanorods: Synthesis and characterization. Ceram Int 44(7):7949–7954
115. Han Z, Fina A (2011) Thermal conductivity of carbon nanotubes and their polymer nanocomposites: A review. Prog Polym Sci 36(7):914–944
116. Joshi P, Upadhyay SH (2014) Evaluation of elastic properties of multi walled carbon nanotube reinforced composite. Comput Mater Sci 81:332–338
117. Kuzumaki T, Miyazawa K, Ichinose H, Ito K (1998) Processing of carbon nanotube reinforced aluminum composite. J Mater Res 13(9):2445–2449
118. Li Q, Rottmair CA, Singer RF (2010) Cnt reinforced light metal composites produced by melt stirring and by high pressure die casting. Compos Sci Technol 70(16):2242–2247
119. Ostovan F, Matori KA, Toozandehjani M, Oskoueian A, Yusoff HM, Yunus R, Ariff AHM, Quah HJ, Lim WF (2015) Effects of cnts content and milling time on mechanical behavior of mwcnt-reinforced aluminum nanocomposites. Mater Chem Phys 166:160–166
120. Khodabakhshi F, Gerlich A, Švec P (2017) Reactive friction-stir processing of an al-mg alloy with introducing multi-walled carbon nano-tubes (mw-cnts): microstructural characteristics and mechanical properties. Mater Charact 131:359–373
121. Huang Y, Li J, Wan L, Meng X, Xie Y (2018) Strengthening and toughening mechanisms of cnts/mg-6zn composites via friction stir processing. Mater Sci Eng A 732:205–211
122. Morisada Y, Fujii H, Nagaoka T, Fukusumi M (2006) Mwcnts/az31 surface composites fabricated by friction stir processing. Mater Sci Eng A 419(1-2):344–348
123. Jamshidijam M, Akbari-Fakhrabadi A, Masoudpanah SM, Hasani GH, Mangalaraja RV (2013) Wear behavior of multiwalled carbon nanotube/az31 composite obtained by friction stir processing. Tribol Trans 56(5):827–832
124. Arab SM, Zebarjad SM, Jahromi SAJ (2017) Fabrication of az31/mwcnts surface metal matrix composites by friction stir processing: Investigation of microstructure and mechanical properties. J Mater Eng Perform 26(11):5366–5374
125. Bagheri B, Abbasi M (2020) Development of az91/sic surface composite by fsp: effect of vibration and process parameters on microstructure and mechanical characteristics. Adv Manuf 8(1):82–96
126. Bagheri B, Abbasi M, Abdollahzadeh A, Kokabi AH (2020) A comparative study between friction stir processing and friction stir vibration processing to develop magnesium surface nanocomposites. Int J Miner Metall Mater 27(8):1133–1146
127. Baradarani F, Mostafapour A, Shalvandi M (2020) Enhanced corrosion behavior and mechanical properties of az91 magnesium alloy developed by ultrasonic-assisted friction stir processing. Mater Corros 71(1):109–117

Publisher's Note